

Characterising cosmic inhomogeneity with anomalous diffusion

D. Kraljic¹

¹ *Rudolf Peierls Centre for Theoretical Physics, University of Oxford, 1 Keble Road, Oxford OX1 3NP, United Kingdom*

19 July 2022

ABSTRACT

Dark matter (DM) clustering at the present epoch is investigated from a fractal viewpoint to determine the scale where the self-similar scaling property of the DM halo distribution transits to homogeneity. Methods based on well-established counts-in-spheres, as well as new methods based on anomalous diffusion and random walks, are applied both to DM halos of the biggest N-Body simulation in the ‘Dark Sky Simulations’ (DS) and an equivalent randomly distributed catalogue. Results for the smaller ‘Millennium Run’ (MR) simulation are revisited. It is found that the MR simulation volume is too small and prone to bias to reliably identify the onset of homogeneity. Transition to homogeneity is defined when the fractal dimension of the clustered and random distributions cannot be distinguished within the associated uncertainties. The “counts-in-spheres” method applied to the DS simulation then yields a homogeneity scale roughly consistent with previous work (~ 150 Mpc/h). The characteristic length-scale for anomalous diffusion to behave homogeneously is found to be at about 250 Mpc/h.

1 INTRODUCTION

The three dimensional distribution of matter observed on the sky exhibits a complex structure of nodes, filaments, walls, and voids. A similar “Cosmic Web” structure appears in N-body DM simulations. Due to the biasing of the luminous matter with respect to the dominant DM component, the knowledge of the distribution of DM in the universe comes mostly from such numerical simulations. This intricate distribution is far from the description used in standard models in cosmology which assumes a Friedmann-Lemaître-Robertson-Walker (FLRW) background with small density perturbations. FLRW assumption is based on the high degree of isotropy inferred from observations of the cosmic microwave background (CMB) (once the dipole is subtracted) and the ‘Copernican Cosmological Principle’ (Clarkson 2012). The inhomogeneities are assumed to be only at small scales, so they should become vanishingly small after averaging over large enough scales, such that the simple description applies. It is therefore important to identify the scale above which the statistical properties of the Universe do not depend on the location. This requires a definition of the notion of the transition to (statistical) homogeneity. It is particularly relevant to searches for the ‘Baryon acoustic oscillation’ (BAO) feature in the two-point correlation function, which is supposed to be present at a comoving scale of 110 Mpc/h in the standard Λ CDM cosmological model. This assumes implicitly that homogeneity has been reached on such scales, so it makes sense only if the homogeneity scale is much smaller than the BAO scale (and the size of the galaxy survey).

One approach to characterise the complex structure in the universe is via fractal analysis. Fractal analysis can also be used to determine the transition to homogeneity in a statistical sense. The analysis has been applied to redshift galaxy surveys: Pan & Coles (2000) to PSCz; Hogg et al. (2005) to SDSS LRG; Sarkar et al. (2009) to SDSS DR6; Scrimgeour et al. (2012) to WiggleZ; Chacón-Cardona & Casas-Miranda (2012b) to SDSS DR9) and to N-Body simulations (Gaité (2010), Chacón-Cardona & Casas-Miranda (2012a)). The quantities of interest are the number of objects within a sphere of radius r , $n(< r)$, and its scaling with r . This is known as a ‘counts-in-spheres’ method. The scaling exponent (or fractal dimension) approaches 3 on the large scales, which is the case for a homogeneous distribution. The transition to homogeneity has been detected for scales of roughly 70 Mpc/h all the way up to 180 Mpc/h or not detected at all (Sylos Labini et al. 2009).

Many different definitions for the transition have been used. Yadav, Bagla & Khandai (2010) define the transition to homogeneity at the point where the clustered distribution scaling exponent cannot be distinguished from the homogeneous one within 1σ uncertainty. The transition, of course, depends on the survey size and intrinsic clustering. They find, for a WMAP5 Λ CDM universe, the upper bound for the transition (according to their definition) to be about 260 Mpc/h.

Another definition for the transition has been developed by Scrimgeour et al. (2012). The definition is insensitive to the statistical error of the scaling exponent, but it arbitrarily chooses the transition to happen when the exponent reaches

arXiv:1410.4107v1 [astro-ph.CO] 15 Oct 2014

to within 1% of the homogeneous value. This enables comparing different surveys at the expense of arbitrariness.

The ‘counts-in-spheres’ method was modified to test cosmic homogeneity with Shannon entropy (Pandey 2013). This made possible a discussion of the finite volume effect of the surveys and the effect of overlapping of the spheres used to measure the scaling dimension. Those effects contribute to the confinement bias (sample of spheres mainly coming from the centre of the survey with lots of overlap), which is especially important for inhomogeneous samples with large fluctuations.

Recent proposals to quantify the structure of the “Cosmic Web” focus on the topology, studying the scale-dependent Betti numbers (van de Weygaert et al. 2013) or the genus statistic (Speare et al. 2013). The topological information can be used as a measure of cosmological parameters (Park & Kim 2010).

This paper extends the methods of fractal analysis to include anomalous diffusion on the DM halo distribution. It also uses one of the biggest N-body simulations to date (Kuhlen, Vogelsberger & Angulo 2012) from the ‘Dark Sky Simulations’ (DS) (Skillman et al. 2014) to avoid and quantify finite volume and overlapping bias, which influence smaller simulations like the ‘Millennium Run’ (MR) simulation (Springel et al. 2005). This paper therefore revisits the result from Chacón-Cardona & Casas-Miranda (2012a), which uses MR simulation data (see Sections 3 and 4). It is found that MR-sized simulations or samples are inadequate to accurately measure the transition to homogeneity.

Diffusion can be modelled as a continuum limit of random walkers on the underlying network (Haus & Kehr 1987). It probes different properties of the underlying point set compared with the ‘counts-in-spheres’ method (Ben-Avraham & Havlin 2000). Anomalous diffusion exhibits a number of scaling exponents (or dimensions) that are different from the normal diffusion and is associated with a fractal structure of the network (Ben-Avraham & Havlin 2000; Sokolov 2011). Thus, it can be used as another characterisation of the distribution of matter. The methods and relevant theoretical background are summarised in Section 2. Section 3 summarises the DS simulation and compares it to the MR simulation. Results for the determination of the fractal exponents and their scale dependence for the ‘counts-in-spheres’ method and methods based on anomalous diffusion are presented in Section 4. The summary of the methods is in the following section.

2 METHODS AND THEORETICAL BACKGROUND

Visual inspection of the distribution of matter in the universe exhibits a self-similar “Cosmic Web” structure of filaments, walls, and voids. A point set (e.g. DM haloes, galaxies) can be characterized via a number of scaling dimensions. Cosmologically, we are interested in the spatial scale above which the transition to a homogeneous distribution occurs, which is determined by scaling dimensions reaching the usual, homogeneous values.

The simplest fractal dimension is the ‘counts-in-spheres’ dimension,

$$n_i(< r) \propto r^{D_i} \quad (1)$$

which counts the number of points within a sphere of radius r centred on the point i with the scaling fractal dimension D_i . An associated quantity, the correlation integral, is defined as in (Bagla, Yadav & Seshadri 2007; Martinez & Saar 2010):

$$C_2(r) = \frac{1}{NM} \sum_{i=1}^M n_i(< r) \quad (2)$$

where N is the total number of points in the distribution (formally $N \rightarrow \infty$) and M is the number of centres on which spheres of radius r have been positioned. This exhibits scaling:

$$C_2 \propto r^{D_2}, \quad D_2 = \frac{\partial \log C_2(r)}{\partial \log r} \quad (3)$$

The deviation of the correlation dimension D_2 from the ambient value D is due to the clustering, as it can be seen in the regime of weak clustering: $D_2(r) \simeq D - D(\bar{\xi}(r) - \xi(r))$ where $\xi(r)$ is the two-point correlation function and $\bar{\xi}(r)$ is its average up to radius r (Bagla, Yadav & Seshadri 2007).

The structure of matter in the Universe is highly irregular and does not exhibit just one simple scaling. Different moments of the correlation integral can be taken to extract more information from the distribution. The generalised correlation integral and dimension are:

$$C_q(r) = \frac{1}{NM} \sum_{i=1}^M n_i^{q-1}(< r), \quad D_q = \frac{\partial \log C_q(r)}{\partial \log r} \quad (4)$$

A simple fractal has just one scaling $D_q = D_2$ at all scales, whereas a multi-fractal has a spectrum of D_q . Positive values of q put more weight on the dense regions whereas negative values on the underdense ones. We can thus extract the scaling behaviour for points mainly located in clusters or voids.

Transition to homogeneity

The correlation dimension D_2 depends on the spatial scale r . In cosmology we are interested in the distance above which the distribution of objects is homogeneous. In the framework of the fractal analysis, this happens when the scaling dimension is equal to the ambient dimension (e.g. $D_2 = 3$). For finite samples, however, the ambient value cannot be reached exactly. Based on Yadav, Bagla & Khandai (2010), a clustered distribution is defined to become homogeneous when $D_2^{clustered}$ cannot be distinguished from $D_2^{unclustered}$ of the unclustered distribution within their errors. That is, $D_2^{unclustered} - D_2^{clustered} = \Delta D_2 \simeq \sigma_{\Delta D_2}$, where $\sigma_{\Delta D_2}$ is the statistical error. This definition is statistically well-motivated. However, the transition evidently depends on the sample size.

The unclustered (or random, or homogeneous) distribution is a distribution of the same size as the clustered sample in terms of the volume and the number of objects, but in which the positions of the objects are random. In what follows the terms “unclustered”, “random”, and “homogeneous” will be used interchangeably.

Diffusion

Normal diffusion

Diffusion on a point set or a network can be modelled with a large number of random walkers. Diffusion is their continuum limit. The walkers jump to neighbouring points from their current position and thus traverse a certain distance, assuming the set of points is embedded in a space that has a notion of distance (e.g. Euclidean space). The standard result for the random walkers (assuming the uncorrelated nature of the walk and no directional bias) is:

$$\langle \mathbf{R}^2 \rangle = \int P(r, t) r^2 d^d \mathbf{r} \propto t \quad (5)$$

$$P(\mathbf{r}, t) = \frac{1}{(4\pi Kt)^{d/2}} \exp\left(-\frac{d r^2}{4Kt}\right) \quad (6)$$

That is, the mean squared displacement scales with the number of steps t and is independent of the dimension d of the Euclidean space. This is a property of normal diffusion.

On a lattice point set the random walker jumps onto the neighbouring points. However, on non-lattice point sets random walkers have to be supplied with the notion of neighbouring points. To have a meaningful long-distance scaling the prescription for the random walker on how to jump to the next point should be limited to short distances. The asymptotic scaling should also be robust against changes in the short-distance prescription. This can be achieved by linking each point to a fixed number of the nearest points, thus creating a network for the walkers. This prescription introduces a slight modification of the scaling law at short distances, while the asymptotic behaviour remains unchanged with respect to the number of nearest points the walker is allowed to jump on.

Anomalous diffusion

A diffusive process is said to be anomalous (Haus & Kehr 1987) if the mean squared displacement grows as:

$$\langle \langle \mathbf{R}_i^2 \rangle \rangle_i \propto t^\alpha \quad (7)$$

with $\alpha \neq 1$. Again, t is the number of steps of the random walker, i the initial position of the walker, and $\langle \cdot \rangle_i$ is the average over positions i . The values with $\alpha < 1$ and $\alpha > 1$ correspond to subdiffusion and superdiffusion.

The advantage of this method is that the anomalous diffusion exponent α is the same ($\alpha = 1$) for homogeneous distributions in any dimension, unlike the 'counts-in-spheres' method which gives $D_2 = 1, 2, 3$ respectively for a homogeneous line, sheet, and volume distribution and does not necessarily imply fractal behaviour (e.g. a galaxy located in a wall would have $D_2 \simeq 2$ but $\alpha \simeq 1$). Similar to the 'counts-in-sphere' method, the homogeneity is reached when $\Delta\alpha(R) \simeq \sigma_{\Delta\alpha(R)}$ at a certain 'radius' R . Note that the effective distance scale here is $\sqrt{\langle r^2 \rangle}$, meaning that the diffusion is sensitive to a range of scales.

Cosmological data (simulated or observed) is limited in volume. Therefore, a diffusion process must be stopped as it reaches the boundaries of the dataset to prevent unphysical leakage (or reflections) of random walkers from the volume. In other words, the whole probability distribution must be contained within the dataset volume to correctly evaluate

the mean distance squared of the random walkers. This imposes an upper bound on the distances probed (smaller than characteristic length-scale of the sample) and makes this method suitable only for large volume datasets.

Conversely one can consider:

$$\langle \langle T \rangle \rangle_i \propto R^{d_w} \quad (8)$$

The walk dimension d_w is defined via the mean number of steps $\langle T \rangle$ that a random walker needs in order to leave a ball of radius R centred on the position i for the first time. This method has a clearly defined scale R , unlike the previously discussed method above that considers the mean square displacement $\sqrt{\langle r^2 \rangle}$. It is comparable to the 'counts-in-spheres' method in terms of efficiency of volume use. For normal diffusion we have $d_w = 2$, and for a mono-fractal with one scaling exponent we have $d_w = 2/\alpha$. Again, the distribution is homogeneous above the radius where $\Delta d_w(R) \simeq \sigma_{\Delta d_w(R)}$.

A fixed number of random walkers start from the initial position. As a consequence, they explore volume at larger distances less efficiently, thus introducing spread relative to shorter distances in the determination of the scaling dimension.

From Eqn. 6 we see that the direct handle on the dimensionality of the underlying Euclidean or fractal space for diffusion is the probability of return $P(\mathbf{0}, t) \propto t^{d_s/2}$, where d_s is the spectral dimension ($d_s = 3$ for a homogeneous three dimensional distribution). This technique is used by Causal Dynamic Triangulation approach to Quantum Gravity (Ambjorn, Jurkiewicz & Loll 2010), where a flow of space time dimension is seen from 2 to 4. However, this approach is difficult to apply on cosmological data that is limited in volume. Random walkers might leak out of the box and never return, thus biasing the probability of return. Also, spatial scale is not present directly. The scale can be indirectly inferred from the diffusion time t , i.e. long/short t corresponds to large/small spatial scale.

3 DARK SKY SIMULATIONS VS MILLENNIUM RUN

Dark Sky (DS) Simulations (Skillman et al. 2014) Early Data Release contains a large volume DM N-Body simulation using $10240^3 \approx 10^{12}$ particles in a volume of $(8.0 \text{ Gpc}/h)^3$ with the Λ CDM cosmology ($\Omega_m = 0.295, \Omega_b = 0.0468, \Omega_\Lambda = 0.705, n_s = 0.969, h = 0.688, \sigma_8 = 0.835$). For reasons of computational efficiency, the halo catalogue obtained using a phase space ROCKSTAR algorithm (Behroozi, Wechsler & Wu 2013) at $z = 0$ is reduced by employing a mass cut $M_{vir} > 10^{12} M_\odot/h$. The resulting catalogue contains $\approx 2.3 \cdot 10^9$ DM halos. The mean number density is $4.6 \cdot 10^{-3}$ halos per $(\text{Mpc}/h)^3$. Equivalently, the mean inter-halo distance is about 6 Mpc.

Millennium Run is a DM N-Body simulation using 10^{10} particles in a $(500 \text{ Mpc}/h)^3$ cubic volume with periodic boundary conditions. Its cosmological parameters are slightly different from the DS simulation ($\Omega_m = 0.25, \Omega_b = 0.045, \Omega_\Lambda = 0.75, n_s = 1, h = 0.73, \sigma_8 = 0.9$). The simulation contains $\approx 1.5 \cdot 10^7$ halos, that is, $1.2 \cdot 10^{-1}$ halos per $(\text{Mpc}/h)^3$ with mean inter-halo distance of approximately

2 Mpc. This means that the shot noise is smaller in the Millennium run simulation compared with the DS simulation.

We can only sample the spheres fully contained in the volume of a simulation in order to avoid the edges. This results in sampling only from the central regions, i.e. the confinement and overlap bias (Pandey 2013; Sylos Labini et al. 2009). Taking many data points from a smaller central subregion artificially brings down the errors and hides the resulting bias. Ideally, for a finite sample, only independent regions should be used. Therefore, much fewer centres can be used (increased errors) and much smaller distances can be probed. For the MR simulation, assuming close-packing, only about 9 independent spheres of radius 140 Mpc/h can be drawn from it, resulting in a big errorbar at such scales. A thousand independent spheres can only be drawn up to about 28 Mpc/h. This should be compared with Chacón-Cardona & Casas-Miranda (2012a), which uses a thousand spheres up to 140 Mpc/h. Furthermore MR uses a 500 Mpc/h box with periodic boundary conditions, meaning that the biggest distance possible between two points is 250 Mpc/h and homogeneity is imposed automatically at this radius. This is at odds with the theoretical expectation in Λ CDM (~ 260 Mpc/h) (Yadav, Bagla & Khandai 2010). Therefore, in order to reliably probe scales ~ 100 Mpc/h, a volume much bigger than the MR simulation is needed.

4 RESULTS AND DISCUSSION

In all the determinations of the scaling exponents' dependence on the radial distance linear fits to the log-log data with bin sizes 15 Mpc/h were used.

Correlation dimension ('counts-in-spheres' method)

A volume of $\approx (8.0 \text{ Gpc/h})^3$ from DS simulation was used to draw a thousand *independent* spheres from it in order to calculate the correlation dimension $D_2(r)$ up to 200 Mpc/h. The same method was applied to a random catalogue of the same size and the same number of points (see Fig. 1). This compares directly to the work done before (Chacón-Cardona & Casas-Miranda 2012a) on the Millennium Run simulation DM halo catalogue, which used a thousand *overlapping* spheres drawn from it. There, $D_2(r)$ could only be determined up to 140 Mpc/h (with the spheres overlapping). Above that radius the systematic bias was obvious (i.e. D_2 exceeded 3, the homogeneous value).

In Fig. 1 we see that the scaling for the random distribution reaches the expected value ($D_2(r) \simeq 3$) at about 40 Mpc/h. Before that radius the effects of discreteness influence the scaling dimension (mean particle separation λ is ~ 6 Mpc/h, so the scaling makes sense at radii $r \gg \lambda$). Hence, the relevant quantity that determines whether a clustered distribution can be distinguished from the random one is $\Delta D_2(r) = D_2^{\text{clustered}}(r) - D_2^{\text{unclustered}}(r)$, which is plotted in Fig. 2.

We see that the transition to homogeneity happens at about 150 Mpc/h, which is comparable to previous work (Chacón-Cardona & Casas-Miranda 2012a).

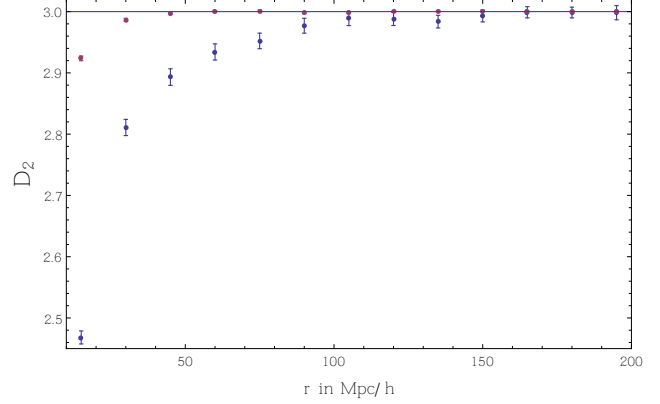


Figure 1. $D_2(r)$ for DS simulation and an equivalent random distribution. The scaling for the random distribution reaches $D_2 = 3$ very quickly. Note that the errorbars for the random distribution are smaller compared to the clustered one.

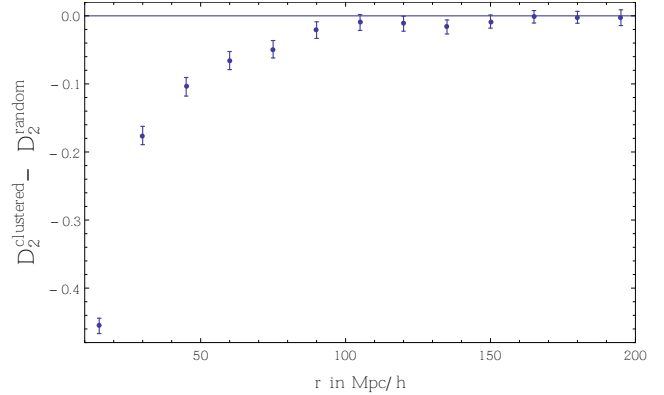


Figure 2. $\Delta D_2 = D_2^{\text{clustered}} - D_2^{\text{random}}$ vs radius in Mpc/h for counts-in-spheres method. The transition to homogeneity happens at around 150 Mpc/h

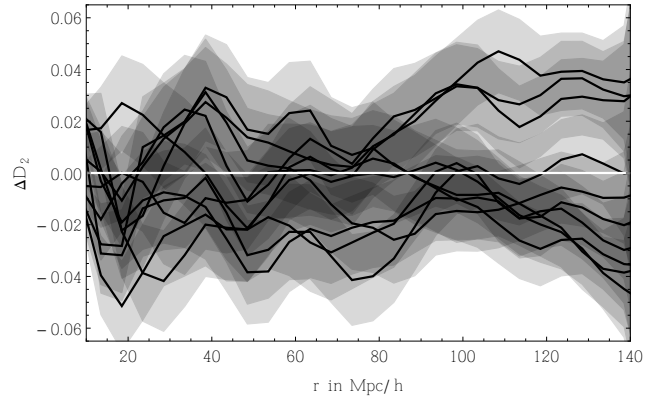


Figure 3. Difference between the counts-in-spheres dimensions, $\Delta D_2 = D_2^{\text{independent}} - D_2^{\text{overlapping}}$, when using a thousand independent spheres in a $(8 \text{ Gpc/h})^3$ DS simulation volume and when using a thousand substantially overlapping spheres each in ten $(0.5 \text{ Gpc/h})^3$ subvolumes of DS. Lines are ΔD_2 and shaded regions are errors ($\approx \pm 0.02$) corresponding to each line.

Overlapping and confinement bias

Previous work (Chacón-Cardona & Casas-Miranda 2012a) determined the counts-in-spheres dimension, D_2 , on the MR simulation by drawing a thousand randomly selected centres from the DM halo distribution that were at least 140 Mpc/h away from the edges of the box. This enabled the determination of D_2 up to radius 140 Mpc/h (‘depth’). However, many of the spheres are overlapping (overlapping bias) and are drawn preferentially from the central part of the box (confinement bias). As mentioned before, sampling of the spheres that overlap significantly also artificially reduces the errorbars.

These effects need to be quantified in order to check whether MR-sized samples can be trusted to precisely and accurately determine the transition to homogeneity using the ‘counts-in-spheres’ method. This was done by randomly selecting a thousand centres in each of 10 MR-sized $\approx (0.5 \text{ Gpc/h})^3$ subvolumes of the DS simulation. The exponent D_2 was determined with depth 140 Mpc/h in each sub-volume. This was then compared to the D_2 exponent deduced by using a thousand centres from the full DS volume where the spheres were independent. In Fig. 3 $\Delta D_2(r) = D_2^{\text{independent}}(r) - D_2^{\text{overlapping}}(r)$ is plotted. We see the systematic offset persist across all scales, also the relevant ones at around 100 Mpc/h. This suggests that volumes as small as the MR simulation are prone to systematic bias of the order of 1%. Hence, the methods to determine the transition to homogeneity either by focussing on the statistical error in the scaling exponent $\sigma_{\Delta D_2}$ Yadav, Bagla & Khandai (2010) or proximity to the theoretical scaling exponent $(D_2 - D)/D = 1\%$ Scrimgeour et al. (2012) cannot be applied reliably. This analysis also shows that the precise shape of the two-point correlation function, which is related to D_2 via $D_2(r) \simeq D - D(\xi(r) - \xi(r))$, is also affected when measured in a MR size simulation or a survey.

Direct comparison of the DS result with the MR result is not easy due to different cosmological parameters used to run the two simulations, different number density of DM particles and the fact that MR uses periodic BC which potentially influence the scales of interest here.

Anomalous diffusion dimensions

The network used for random walkers was constructed in such a way that each DM halo had a neighbourhood of twelve nearest halos. The construction of the network is computationally expensive, especially for large catalogues. Additionally, the links that were farther than 20 Mpc/h were rejected in order to keep short-distance effects from influencing the long-distance scaling. This lower ‘cut-off’ provides a separation of small scales from the large ones that are of interest here. However, together with the discreteness of the data, the ‘cut-off’ introduces spurious effects at smaller scales which can be seen for the diffusion on the unclustered random distribution of halos (see Fig. 4 and Fig. 7). Note how the scaling for the random distribution approaches the expected theoretical values. To correct for this spurious effect, the difference of scaling exponents between the clustered and unclustered distributions is taken as relevant for the study of the transition to homogeneity.

The analysis was repeated for a network constructed by

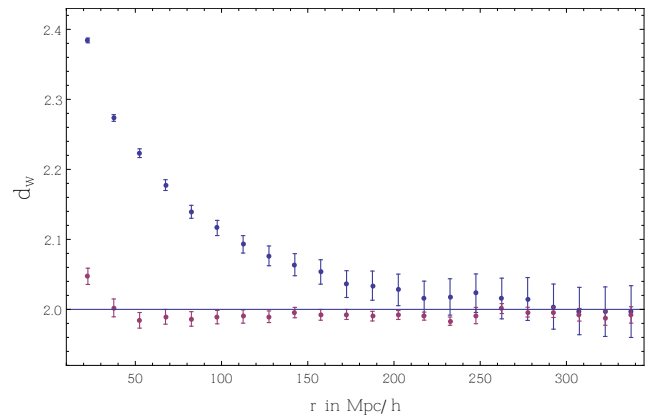


Figure 4. $d_W(r)$ for DS and equivalent implementation on a random catalogue. The small scale effects of the implementation of the random walkers is seen in the lower set of points (random catalogue). Anomalous diffusion persists beyond 200 Mpc/h in the clustered distribution.

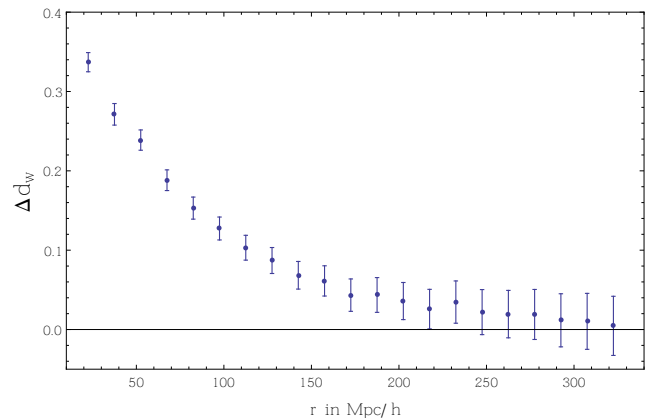


Figure 5. $\Delta d_W = d_W^{\text{clustered}} - d_W^{\text{unclustered}}$ between the DS sample and a random distribution for the implementation where the neighbourhood of each halo is the twelve nearest haloes.

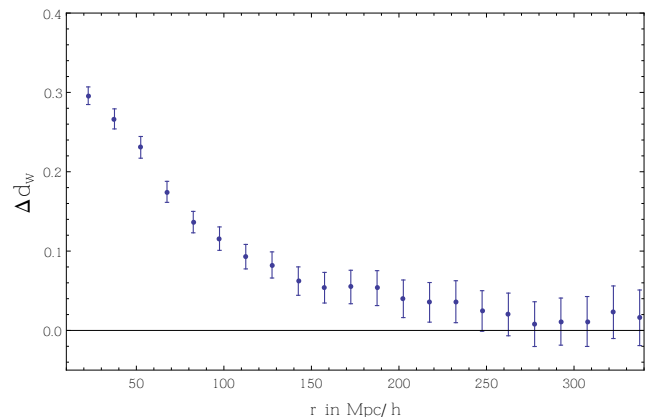


Figure 6. $\Delta d_W = d_W^{\text{clustered}} - d_W^{\text{unclustered}}$ between the DS sample and a random distribution for the implementation where the neighbourhood of each halo is the nearest eighteen haloes.

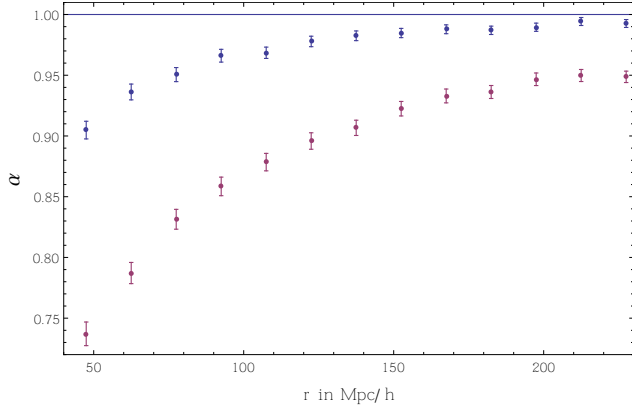


Figure 7. Mean square displacement scaling $\alpha(r)$ for a random distribution (upper set of points) and DS for the implementation where the neighbourhood of each halo is the nearest twelve haloes.

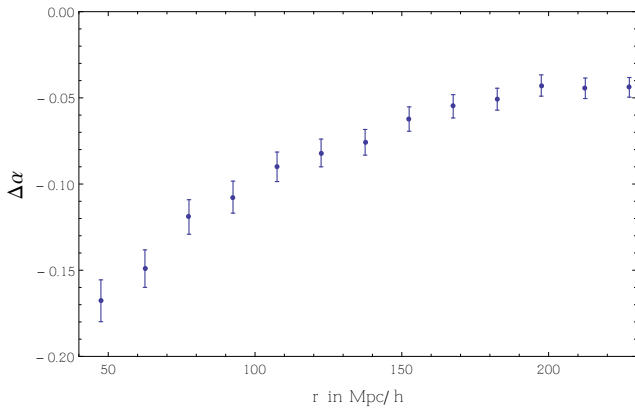


Figure 8. $\Delta\alpha = \alpha^{clustered} - \alpha^{unclustered}$ between the DS sample and a random distribution for the implementation where the neighbourhood of each halo is the nearest twelve haloes.

connecting each halo to the eighteen nearest halos. This was done in order to check that the results for the scaling dimensions did not substantially depend on such a choice (compare Figs. 5, 6 and Figs. 8, 9). Naturally, some differences are expected at smaller scales due to spurious discreteness effects.

The method was applied to a set of lattice distributions and deterministic fractal distributions with known scaling exponents in order to confirm that the implementation of the diffusive process gave correct asymptotic scaling exponents.

The number of walkers for each starting point is chosen to be very large in order for the walkers to saturate the possible ways of exploring a given volume starting from a specific point. Thus, the spread in the scaling exponent comes dominantly from having different points used as centres for the random walkers.

Mean square displacement scaling α

Scaling of the mean distance squared with the number of steps, $\langle r^2 \rangle \propto t^\alpha$, up to an effective radius ($\sqrt{\langle r^2 \rangle}$) of 220 Mpc/h, was explored. The number of starting centres for the random walkers was 512 in independent volumes and care was taken to make sure that the diffusion processes were

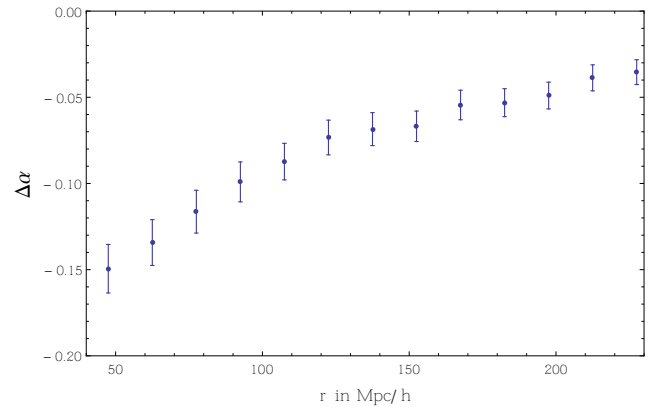


Figure 9. $\Delta\alpha = \alpha^{clustered} - \alpha^{unclustered}$ between the DS sample and a random distribution for the implementation where the neighbourhood of each halo is the nearest eighteen haloes.

terminated before leaking out of the volume available or before overlapping.

This is a less efficient method in terms of using the available volume compared to the ‘counts-in-spheres’ method. The reason is that, in order to evaluate the scaling exponent α , all the random walkers for a given number of steps t_0 are needed. Hence, the diffusive process extends over a range of scales (with the characteristic scale $\sqrt{\langle r^2(t_0) \rangle}$ much smaller than $|\mathbf{r}_{max}(t_0)|$). As a result, the transition to homogeneity happens slowly as the notion of scale is spread out (see Figs. 7 8 and 9). This explains the lack of convergence of the clustered distribution to the random one up to $\sqrt{\langle r^2 \rangle} \sim 220$ Mpc/h.

Walk dimension d_w

Scaling of the mean number of steps needed to leave a ball of radius R , $\langle T \rangle \propto R^{d_w}$, was determined up to 350 Mpc/h. As the radius R grows a smaller number of independent centres is available. The same volume of $(8.0 \text{ Gpc/h})^3$ as in the ‘counts-in-spheres’ method was used (same efficiency of volume use). This enables a direct comparison of the results and the errorbars. The distance scale for this diffusive process is well-defined, contrary to the method measuring α discussed above. This can be seen from the walk dimension d_w and anomalous diffusion dimension α for the unclustered distribution in Figs. 4, 7. The walk dimension, d_w , converges to the theoretically expected value at about 50 Mpc/h whereas α takes longer. The transition to homogeneity via anomalous diffusion, as defined in Sec. 2, happens at a different, larger scale (above 250 Mpc/h) than for the ‘counts-in-spheres’ method (see Figs. 4 5 6).

It is useful to check how sensitive the walk dimension d_w is to the transition to homogeneity. This is done by randomly selecting subvolumes of the DS simulation with the box lengths being 100 Mpc/h and imposing periodic boundary conditions. In Fig. 10 we see that the transition to homogeneity does begin at about 100 Mpc/h. This should be compared with Fig. 4, where the transition happens later, as described above.

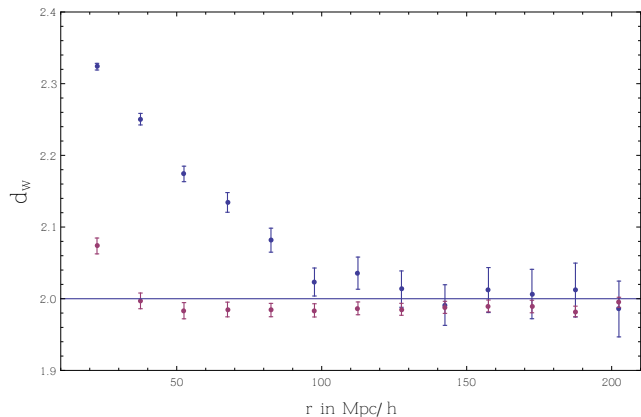


Figure 10. $d_W(r)$ for the case where the homogeneity is artificially imposed at 100 Mpc/h. The lower set of points corresponds to the unclustered distribution.

Fractal analysis and phase information

The ‘counts-in-spheres’ method has been used to test the assumption of homogeneity and determine the transition to it. The method, despite being inspired by fractal analysis, cannot characterise the intricate fractal-like structure of the ‘Cosmic Web’. The reason is that the ‘counts-in-spheres’ method, provided the homogeneity is reached in the sample, only contains the information about the two-point correlation function or equivalently the power spectrum (Bagla, Yadav & Seshadri 2007). This means that the phase information of the density field which is responsible for the filamentary structures is lost.

Following (Chiang 2001; Coles 2003), the phases of the Fourier transform of the density field obtained from the DS halo catalogue, $\delta_{\mathbf{k}}$, were shuffled. This erases the phase information but preserves the power spectrum that depends only on the square of the density field $|\delta_{\mathbf{k}}|^2$. The density field with shuffled phases was then used to generate a discrete distribution of points, i.e. a halo catalogue. This was done by Poisson sampling from the phase-shuffled density field. That is, in a volume V , the number of selected points is proportional to the enclosed mass $\langle N(V) \rangle \propto M(V)$. The total number of points selected is such that the same overall number density as in the DS catalogue is achieved. The difference between the density field from the DS simulation and the phase-shuffled field is illustrated at the top of Fig. 11.

The $D_2(r)$ determined in the generated catalogue is the same (within the errors) as in the original DS halo catalogue. The changes in the scaling exponents for the diffusive processes can be checked as well. In Fig. 11, we see that the difference between the $d_W(r)$ for the original and the shuffled distribution shows systematic deviation above 100 Mpc/h. However, ascertaining the difference more precisely (i.e. decrease the errorbars) would require vastly more computational resources. At smaller scales, the difference in $d_W(r)$ is due to small scale effects coming from the process of obtaining a discrete representation of the phase-shuffled density field.

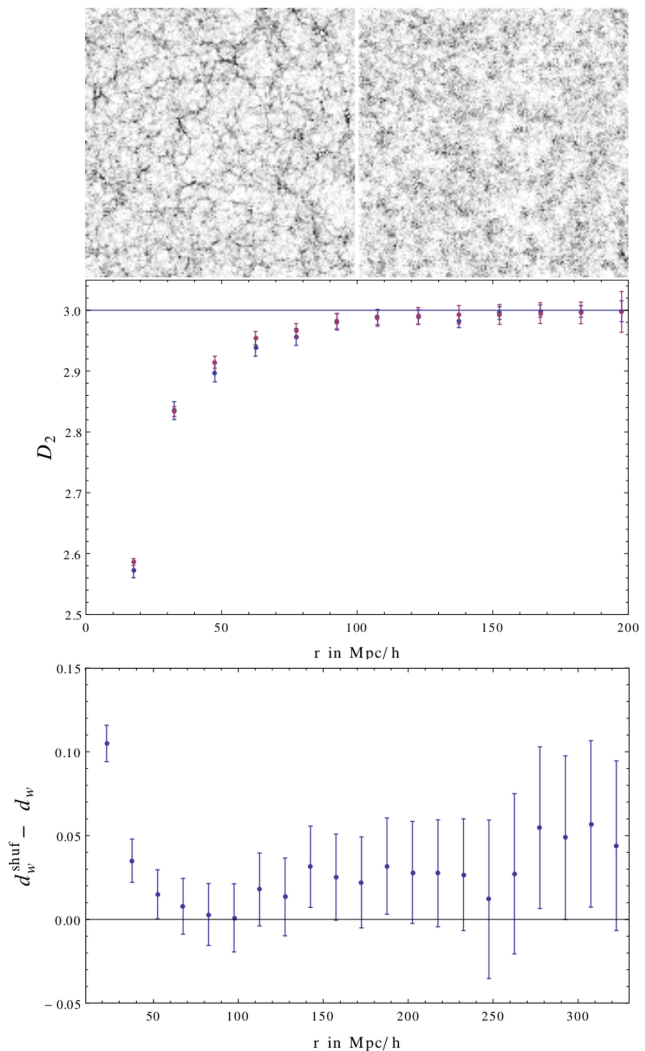


Figure 11. Comparison of the DS halo catalogue and the phase-shuffled catalogue obtained from it. Top left is a $600 \times 600 \times 10$ (Mpc/h)³ slice through the DS catalogue. Top right is a slice through its corresponding phase-shuffled catalogue. The middle shows $D_2(r)$ where purple points are the phase-shuffled case and blue points are the original data. The bottom is $\Delta d_W(r) = d_W^{shuf}(r) - d_W(r)$.

CONCLUSIONS

This paper presents a novel way of characterising the distribution of matter in the universe based on the ideas of anomalous diffusion. The methods were tested on a DM halo catalogue from the biggest of the ‘Dark Sky Simulations’ (DS), a very large N-body simulation of volume $(8 \text{ Gpc/h})^3$. Diffusion was modelled by performing random walks on the set of halos. The underlying distribution can be described by scaling exponents for various diffusive processes. Determination of the values of the scaling exponents and their dependence on the distance scale can be used to decide whether a particular distribution can be distinguished from the homogeneous one.

We measure the mean time $\langle T \rangle$ for a random walker to leave a ball of radius R , and how it scales with the radius: $\langle T \rangle \propto R^{d_w}$. In terms of efficiency of volume use, this method

is comparable to the ‘counts-in-spheres’ method, which has been extensively used in the past to characterise the distribution of matter in the universe. For an explicitly homogeneous distribution (i.e. random, unclustered) we find quick convergence of d_W to the theoretically expected value, namely $d_W \simeq 2$. For the diffusion on the DS distribution of halos we find the convergence of the scaling exponent d_W to the homogeneous value to be at about 250 Mpc/h. This characteristic distance can then be measured and compared in different surveys and N-body simulations.

We also measured how the RMS distance traversed by a random walker scales with the number of steps, $\langle r^2 \rangle \propto t^\alpha$. The notion of distance here is only effective, $\sqrt{\langle r^2 \rangle}$, and therefore sensitive to a range of scales. Unsurprisingly the convergence of the scaling exponent α to the homogeneous values is slow. Measuring α probes shorter distance scales compared to the method above in a finite volume sample and is less efficient in the use of the available volume.

The size of the DS simulation also enables quantification of the bias in the determination of the ‘counts-in-spheres’ fractal dimension when smaller volumes are used. As the radius of the sphere used for the counts-in-spheres method approaches the survey size, only central regions are preferentially sampled (confinement bias) in order to avoid edge effects. This leads to substantial overlap of the spheres used and artificial reduction of errorbars. We show that Millennium Run sized volumes that have been used in previous studies of the ‘counts-in-spheres’ fractal dimension are not sufficiently big to precisely and accurately determine the transition to homogeneity, irrespective of the exact definition when transition happens.

ACKNOWLEDGEMENTS

The author is supported by the STFC and would like to thank Subir Sarkar for useful discussions and comments on the draft.

REFERENCES

- Ambjorn J., Jurkiewicz J., Loll R., 2010, 321
 Anderson L., et al., 2013
 Bagla J., Yadav J., Seshadri T., 2007, Mon.Not.Roy.Astron.Soc., 390, 829
 Behroozi P. S., Wechsler R. H., Wu H.-Y., 2013, ApJ, 762, 109
 Ben-Avraham D., Havlin S., 2000, Diffusion and reactions in fractals and disordered systems. Cambridge University Press
 Chacón-Cardona C. A., Casas-Miranda R. A., 2012a, MNRAS, 427, 2613
 Chacón-Cardona C. A., Casas-Miranda R. A., 2012b, ArXiv e-prints
 Chiang L.-Y., 2001, MNRAS, 325, 405
 Clarkson C., 2012, Comptes Rendus Physique, 13, 682
 Coles P., 2003, Statistical Properties of Cosmological Fluctuations, Sánchez N. G., Parijskij Y. N., eds., Kluwer Academic Publishers, p. 237
 Gabrielli A., Labini F. S., Joyce M., Pietronero L., 2005, Statistical physics for cosmic structures. Springer
 Gaite J., 2010, J. Cosmology Astropart. Phys., 3, 6
 Gaite J. C., 2007, Astrophys.J., 658, 11
 Haus J. W., Kehr K. W., 1987, Phys Reps, 150, 263
 Hogg D. W., Eisenstein D. J., Blanton M. R., Bahcall N. A., Brinkmann J., et al., 2005, Astrophys.J., 624, 54
 Kim J., Park C., Rossi G., Lee S. M., Gott, III J. R., 2011, Journal of Korean Astronomical Society, 44, 217
 Kuhlen M., Vogelsberger M., Angulo R., 2012, Physics of the Dark Universe, 1, 50
 Labini F. S., 2010, AIP Conf.Proc., 1241, 981
 Martinez V. J., Saar E., 2010, Statistics of the galaxy distribution. CRC Press
 Nadathur S., 2013, MNRAS, 434, 398
 Nadathur S., Hotchkiss S., 2013, ArXiv e-prints
 Pan D. C., Vogeley M. S., Hoyle F., Choi Y.-Y., Park C., 2012, MNRAS, 421, 926
 Pan J., Coles P., 2000, Mon.Not.Roy.Astron.Soc., 318, L51
 Pandey B., 2013, MNRAS, 430, 3376
 Park C., Kim Y.-R., 2010, ApJ, 715, L185
 Sarkar P., Yadav J., Pandey B., Bharadwaj S., 2009
 Scrimgeour M., Davis T., Blake C., James J. B., Poole G., et al., 2012, Mon.Not.Roy.Astron.Soc., 425, 116
 Skillman S. W., Warren M. S., Turk M. J., Wechsler R. H., Holz D. E., Sutter P. M., 2014, ArXiv e-prints
 Sokolov I., , in Meyers R. A., ed., , Mathematics of Complexity and Dynamical Systems. Springer New York, pp 13–25
 Speare R., Gott J. R., Kim J., Park C., 2013, ArXiv e-prints
 Springel V. et al., 2005, Nature, 435, 629
 Sylos Labini F., 2011, Classical and Quantum Gravity, 28, 164003
 Sylos Labini F., Vasilyev N. L., Pietronero L., Baryshev Y. V., 2009, EPL (Europhysics Letters), 86, 49001
 van de Weygaert R. et al., 2013, ArXiv e-prints
 Yadav J. K., Bagla J., Khandai N., 2010, Mon.Not.Roy.Astron.Soc., 405, 2009